PCCP

Accepted Manuscript

ROYAL SOCIETY OF CHEMISTRY

www.rsc.org/pccp

PCCP

RSCPublishing

ARTICLE

Band gap narrowing in nitrogen-doped $La_2Ti_2O_7$ predicated by density-functional theory calculation

Cite this: DOI: 10.1039/x0xx00000x

Junying Zhang*[a], Wenqiang Dang[a], Zhimin Ao[b], Scott K. Cushing[c] and Nianqiang Wu*[c]

Received 11th January 2015,
Accepted

DOI: 10.1039/x0xx00000x

www.rsc.org/

In order to reveal the origin of enhanced photocatalytic activity of N-doped $La_2Ti_2O_7$ in both the visible light and the ultraviolet light regions, its electronic structure has been studied using the spin-polarized density functional theory (DFT) and the Heyd-Scuseria-Ernzerhof (HSE06) hybrid approach in this work. The results show that the deep localized states are formed in the forbidden band when nitrogen solely substitutes for oxygen. Introducing the interstitial Ti atom into the N-doped $La_2Ti_2O_7$ photocatalyst still causes the presence of localized energy band. Two nitrogen substitutes co-exist stably with one oxygen vacancy, creating a continuum energy band just above the valence band maximum. The formation of a continuum band instead of mid-gap states can extend the light absorption to the visible light region without increasing the charge recombination, explaining the enhanced visible light performance without deteriorating the ultraviolet light photocatalytic activity.

1. Introduction

Since discovery of photocatalysis by Fujishima and Honda[1], semiconductor-based materials have been found wide applications in removing organic pollutants from water and air, splitting water into hydrogen and oxygen, as well as reducing CO_2[2-4]. Of the numerous photocatalysts, layer-structured semiconductors have received extensive attention because the reduction and oxidation reactions, *e.g*. H_2 and O_2 evolution sites, are separated out[5-7]. Perovskite-type photocatalysts consist of the network of corner-sharing octahedra that benefit to the mobility of charge carriers, leading to high photocatalytic activity[8-10]. Perovskite-type $La_2Ti_2O_7$ with a layered structure possesses the merits of both perovskite and layered structures, which exhibits high photocatalytic activity toward organic decomposition, water splitting and CO_2 reduction. For example, layered perovskite $La_2Ti_2O_7$ (110) loaded with nickels showed a quantum yield as high as 12% in water splitting under ultraviolet (UV) irradiation, which exhibited much better photocatalytic activity than Pt-loaded TiO_2.[5] In the absence of a co-catalyst, $La_2Ti_2O_7$ nanosheets demonstrated similar activity to Degussa P25 in photocatalytic hydrogen evolution from the water–ethanol solution[11]. It has also been reported that 98% Cr(VI) ions in water was removed by $La_2Ti_2O_7$ after 3 hours of UV irradiation[12].

$La_2Ti_2O_7$ has a wide band gap (~4.0 eV), which depends on the synthesis method and the resulting morphology.[5,11,13-19] Hence it shows photocatalytic activity only under UV light irradiation. Rh-doped $La_2Ti_2O_7$ was active for H_2 evolution from an aqueous methanol solution under visible light irradiation owing to the photo-excitation of localized energy levels resulting from the Rh^{3+}doping[14]. Similarly, Cr and/or Fe doping in $La_2Ti_2O_7$ induced intensive light absorption in the visible light region and photocatalytic hydrogen production from the water–methanol solution due to the formation of a partially filled 3d band in the band gap[17,20]. The recent experimental results demonstrated that the nitrogen-doped $La_2Ti_2O_7$ nanosheets not only showed significant visible light photocatalytic activity but also exhibited enhanced ultraviolet light photocatalytic activity[13,21]. Nitrogen doping in $La_2Ti_2O_7$ narrowed the band gap rather than creating the localized mid-gap states, which was different from N-doped anatase TiO_2. These results could not be explained by the first-principles calculations, which showed that nitrogen substituting for oxygen caused the formation of the localized energy band in the band gap of $La_2Ti_2O_7$ [22, 23]. Since the energy band gap is a critical factor governing the photocatalytic activity; and doping is the most common method for altering the energy band gap[2], it is essential to understand the effect of doping on the electronic band structure of a semiconductor.

Herein, we investigate the influence of N-doping on the crystal and the electronic structures of $La_2Ti_2O_7$ using first-principles calculations. We assume that nitrogen substitutes for oxygen when it is doped in $La_2Ti_2O_7$ based on the experimental evidence[13]. We check whether the deep states will be formed in the forbidden band when nitrogen solely replaces oxygen. We also examine whether a localized energy band will still exist when the nitrogen substitutes co-exist with an interstitial Ti atom. Furthermore, we explore how the oxygen vacancies are used to stabilize the dopants, leading to an enhancement of visible light absorption without reducing the charge carrier lifetime. In particular, we investigate what is the case if one oxygen vacancy (V_O) stably exists with two nitrogen substitutes (N_S).

2. Calculation methods

The calculations have been performed using the Vienna ab-initio simulation program (VASP)[24]. Adopting Perdew-Burke-Ernzerhof

(PBE) prescription, the generalized gradient approximation (GGA) was used to represent the electronic exchange-correlation energy during the geometry relaxation [25]. Hybrid-functional Heyd-Scuseria-Ernzerhof (HSE06) method[26] was also employed to calculate the electronic structure. The projector-augmented-wave (PAW) potentials were used to describe the electron-ion interaction[27]. The valence configurations including valence and semicore electrons were $2s^2 2p^4$ for oxygen, $2s^2 2p^3$ for nitrogen, $3p^6 3d^3 4s^1$ for titanium and $5s^2 5p^6 5d^1 6s^2$ for lanthanum. The cut-off energy was 450 eV and the Monkhorst-Pack k-point mesh was 6×8×4 for a 44-atom supercell. Structural relaxations were performed until the self-consistent total energy difference reached 10^{-5} eV and the residual forces on atoms fallen below 0.02 eV/Å.

3. Results and Discussion

The monoclinic $La_2Ti_2O_7$ has a layered perovskite structure with *P21* space group. The calculated lattice parameters using GGA are respectively a = 7.795 Å, b = 5.604 Å and c = 13.264 Å (Fig.1(a)), agreeing well with the experimental values of a = 7.812 Å, b = 5.5440 Å, and c = 13.010 Å [28]. For the supercell containing 44 atoms, there were 14 lattice sites of oxygen atom for nitrogen to enter, giving rise to a doping concentration of 3.6 at% similar to the experimental value [13]. We calculated the total energies for all the 14 configurations, and the relaxed geometry with the minimum total energy is shown in Fig.1(b). It can be seen that doping N into $La_2Ti_2O_7$ had little influence on the crystal structure.

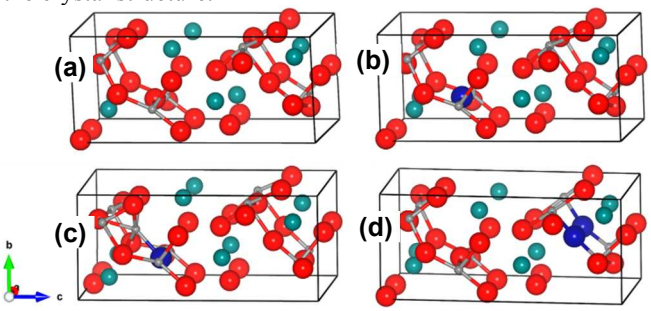

Fig.1 Supercells showing the optimized crystal structure of pristine (a), N-doped $La_2Ti_2O_7$ (b), $La_2Ti_2O_7$ with complex $Ns+Ti_i$ (c) and $La_2Ti_2O_7$ with complex defects ($2N_s + V_o$) (d). The grey, red, light-blue and blue spheres denote the Ti, O, La, and N atoms, respectively.

Fig.2 shows the density of states (DOS) of pristine $La_2Ti_2O_7$ resulting from the calculations of DFT and HSE06 hybrid function. It can be seen that the components of the DOS curves obtained with the two methods were very similar. The valence band maximum was composed of O 2p in majority and of Ti 3p, Ti 3d and La 5p, La 5d in minority. The conduction band minimum was mainly constructed by Ti 3d with minor O 2p and few La 5d states. Since all the elements contribute to the valence band maximum (VBM) and the conduction band minimum (CBM), the subtle stoichiometric change, *e.g* by doping other elements, forming the vacancies or interstitial atoms, will definitely affect the electronic structure of the system.

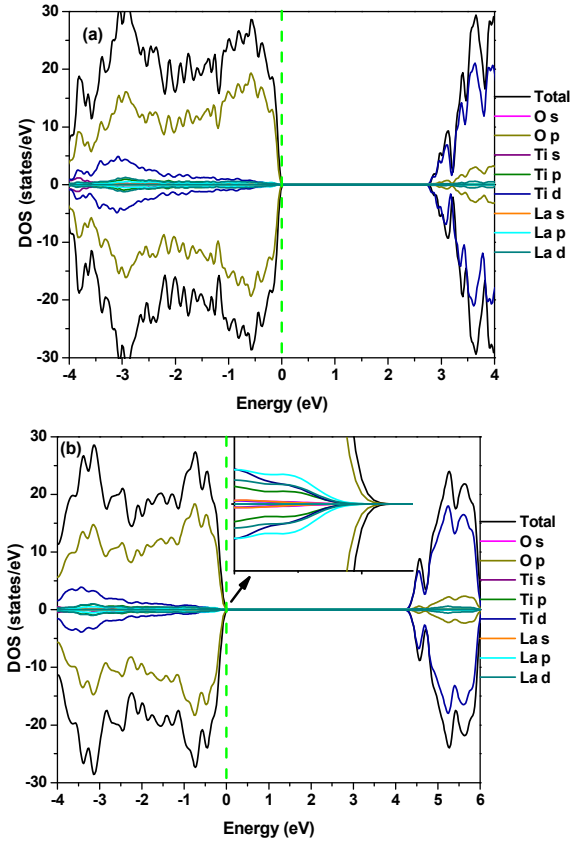

Fig.2 DOS of pristine $La_2Ti_2O_7$ calculated with DFT (a) and HSE06 method (b). The dash line annotates the Fermi level.

The indirect band gap of pristine $La_2Ti_2O_7$ calculated with DFT was 2.9 eV (Fig.3 (a)), underestimating the experimental value due to well-known limitations in DFT [29, 30]. When HSE06 hybrid method was used, the calculated band gap was 4.4 eV (Fig.3(b)), which was slightly larger than the typical experimental value obtained with the solid-state reaction (3.8 eV)[14] and the molten salt synthesis method (3.9 eV)[15].

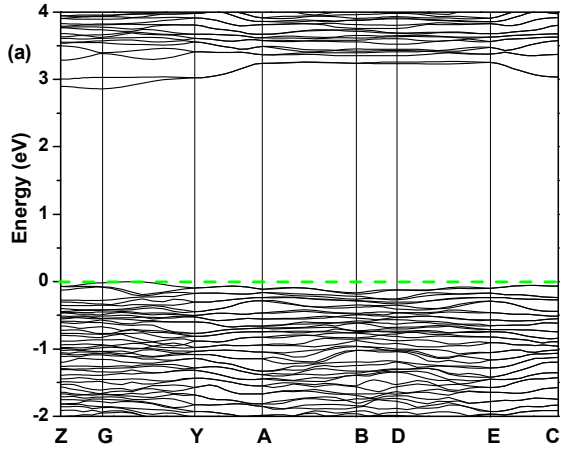

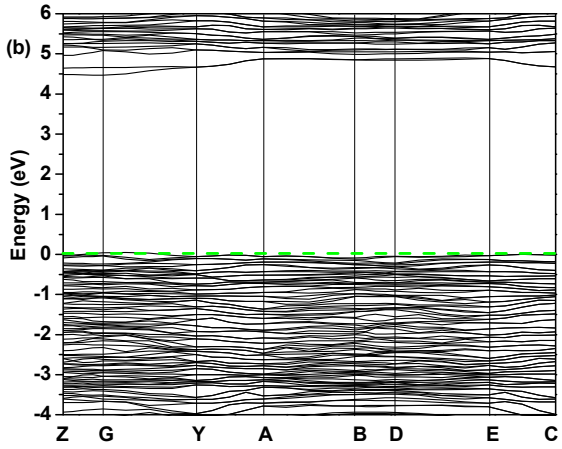

Fig.3 Band structure of pristine $La_2Ti_2O_7$ calculated with DFT (a) and HSE06 method (b). The dash line annotates the Fermi level.

Fig.4 and Fig.S1 reveal the DOS and band structure of N-doped $La_2Ti_2O_7$. The zero energy point was set to the Fermi level of pristine $La_2Ti_2O_7$. The systems with defects were corrected by aligning the average electrostatic potential (V_{av}) of La, Ti and O atoms located far from the defects and the V_{av} for the same elements in the pristine $La_2Ti_2O_7$ [31]. When N substituted for O to form the N_S defect, the localized deep energy states appeared in the middle of the forbidden band, which came from the mixture of N 2p, O 2p, Ti 3d and La 5d orbitals. Furthermore, Fig.4(c) shows that the Ti d orbitals were hybridized with the N p orbitals at VBM. As a result, mixing of N, O, Ti and La orbitals caused the add-on shallow states above the VBM. Band gap narrowing of 0.30 eV and 0.41 eV occurred in comparison with the pristine material, respectively, for the value calculated using DFT and HSE06 methods. The N_S defect shifted the direct transition at the G point to a similar energy as the indirect transition near the B and D point, comparing Fig.3 with Fig. 4, allowing a larger increase in absorption near the band edge. Since N requires one more electron than an O atom from the $La_2Ti_2O_7$ lattice, the unequal up and down-spin electrons result in the asymmetric DOS curve. These results agreed with the previous results calculated using HSE06 method[22,23]. In TiO_2, first-principle calculations also showed that N_S produced the deep localized states in the band gap[32-34], similar to the results in this work. The deep localized energy band was the un-occupied state. It can induce the limited visible light photocatalytic activity but it generally has an adverse effect on the UV light photocatalytic activity since the mid-gap states can act as the charge traps[35].

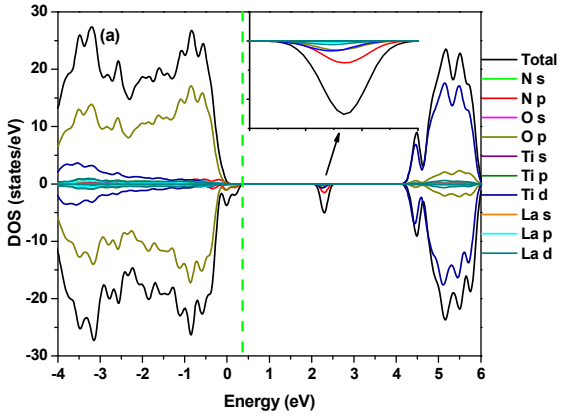

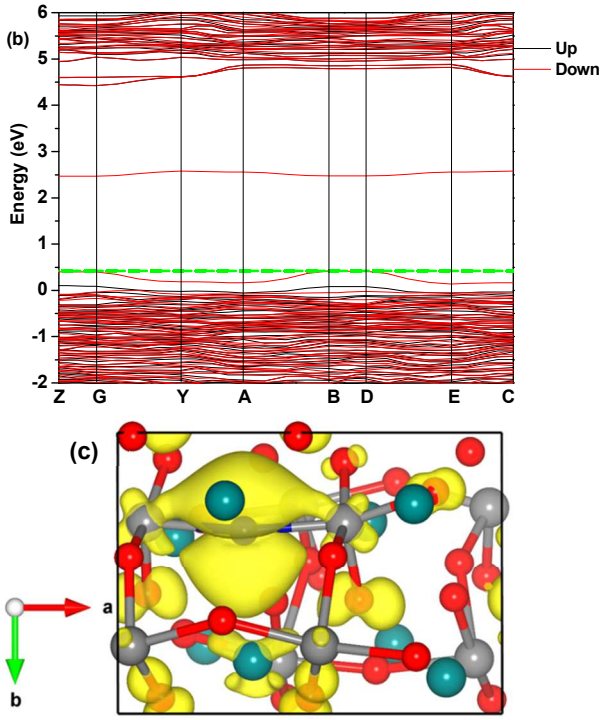

Fig.4 DOS (a), band structure (b) and partial electron density of the VBM at a 0.01 eV/Å^3 isosurface level (c) of $La_2Ti_2O_7$ with the N_S defect calculated using HSE06 method. The dash line annotates the Fermi level.

Recently, the DFT plus the onsite Coulomb interaction (U) calculation shows that a N_S is strongly bound with a titanium atom at interstitial site (Ti_i), giving rise to defect-impurity band thermally connected with the host VBM and eliminating the localized N_S-related states[31]. The suggested model mechanism gives a reasonable explanation for the photocatalytic oxidation reactions as well as the red-shift of the light absorption edge observed in N-doped TiO_2. In this $La_2Ti_2O_7$ system, we also investigated the electronic structure when N_S and Ti_i were bound together to form a complex defect. One Ti atom is inserted into the largest interstitial site in the 44-atom supercell so as to bring minimum lattice distortion to the system, as shown in Fig.1(c). The point-defect formation energy was calculated using the formula:

$$E_{form} = E_D - E_H + \sum_i a_i n_i \mu_i \quad (1)$$

where E_{form} is the point-defect formation energy, E_D is the total energy of the system containing point-defects, E_H is the total energy of the pristine system, a_i = -1 or 1 if an i atom is added or removed, n_i is the number of the i atom, and μ_i is the chemical potential of the i atom calculated using the method as shown in the supporting information.

The formation energy of $Ns+Ti_i$ is plotted in Fig.S2. It can be seen that under the O-poor and Ti-rich condition, the formation energy is negative, which indicates that the N dopant and the interstitial Ti atoms are prone to co-exist. The formation energy comparison in Fig.S3 also indicates that forming interstitial Ti atom is energetically favourable when one oxygen atom is substituted by nitrogen atom in the O-poor condition.

When N_s and Ti_i co-existed, the electronic structures calculated using HSE06 hybrid method were very similar to the model where N solely doped $La_2Ti_2O_7$, *i.e.*, localized mid-gap states formed as

shown in Fig.5 and Fig.S4. According to the hybrid results, the two localized energy bands, composed of mainly Ti 3d and least O 2p states, covered a large range below the CBM, unlike the system with only the N_s defect where one deep energy band lies in the middle of the band gap. Furthermore, the mixed N 2p and O 2p energy band (denoted by L_1) was located 0.4 eV above the VBM, rather than being close to the VBM as in the N mono-doped system. The hybridization among the N p and Ti d orbitals can be clearly observed using the partial electron densities in Figs. 5(c) and 5(d). The localized energy bands were occupied, thus the Fermi level was substantially upraised to just below the CBM. Again, the deep localized mid-gap energy bands (denoted by L2) lead to low charge mobility and can act as the charge-carrier traps, which is unfavourable to the photocatalytic activity[35]. The DOS and the band structure obtained with DFT also indicated the formation of localized energy band 0.3 eV above the VBM (Fig.S4).

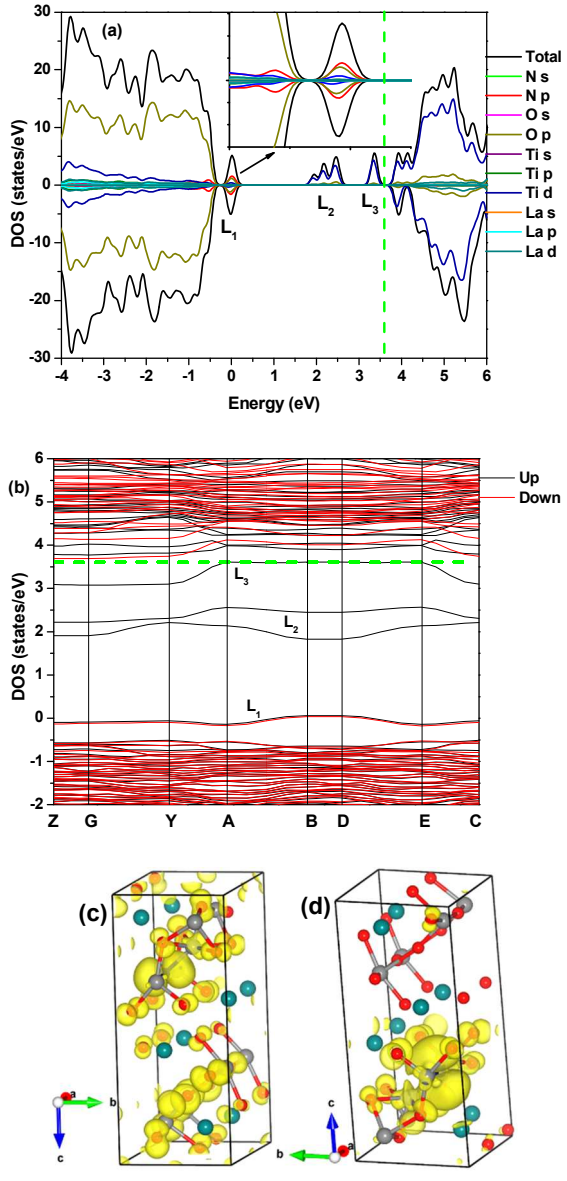

Fig.5 DOS (a), band structure (b), the partial electron densities of the VBM (c) and of the localized energy level (L1) at point D (d) at a 0.01 eV/Å^3 isosurface level of $La_2Ti_2O_7$ with the N_s and the Ti_i defects in a supercell calculated using HSE06 method. The dash line annotates the Fermi level.

Both DFT-calculations and experiments have showed that nitrogen doping leads to formation of oxygen vacancies in bulk TiO_2[36, 37]. The complex defects (N_s +V_o) alter the band gap, also cause the formation of a localized energy band mid-gap[35,38,39]. The 3d states of Ti^{3+} below the conduction band, which are associated with oxygen vacancies, have been found to act as the electron-hole recombination sites, leading to the reduction of photocatalytic activity[35]. Herein we also found that the formation energy was substantially reduced after V_O was introduced into the N-doped $La_2Ti_2O_7$ lattice (Fig. s3), which indicated that oxygen vacancies were easily formed during the introduction of N into the lattice. But the complex defects influence on the electronic structures was greatly different for $La_2Ti_2O_7$ and TiO_2. In order to achieve the electrical neutrality, the model was built to contain two N_S and one V_O (Fig.1 (d)). As shown in Fig.6 and Fig.S5, the localized energy band completely disappeared when two N_S co-existed with one V_O. The mixed N 2p, O 2p and Ti 3d formed a continual energy band on the top of the valence band (obtained by HSE06 method) or thermally connect with VBM (obtained by DFT), which accounted for the parallel red shift of the whole optical absorption edge of the N-doped sample[13]. The band gap was narrowed by 0.85 eV and 1.15 eV, which were determined by the DFT and the HSE06 approaches, respectively. For the HSE06 calculation result, the VBM shifted upwards by 1.07 eV while the CBM shifted downwards by 0.14 eV in comparison with pristine $La_2Ti_2O_7$. The VBM and CBM variation trends obtained by the theoretical calculation were consistent well with the experimental result reported for the N-doped $La_2Ti_2O_7$ nanosheets[13]. As well, the added bands created a broad direct transition at a similar energy as the indirect band gap, improving the light absorption. This was in agreement with the added band edge as seen experimentally with N doping in $La_2Ti_2O_7$, wherein the absorption can be described by a superimposed direct and indirect gap[13,21].

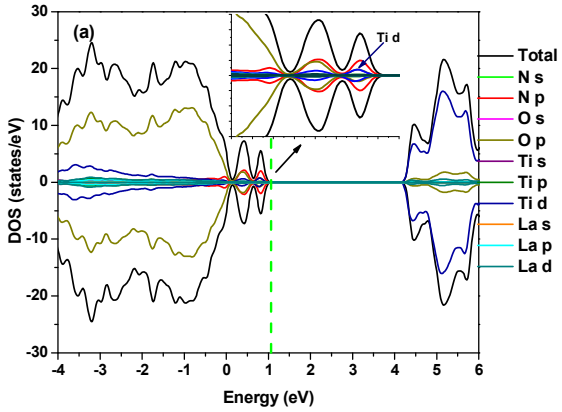

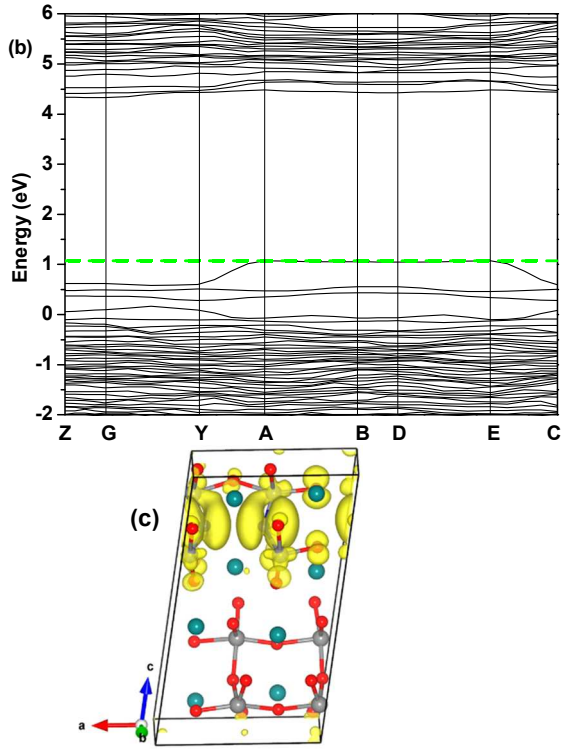

Fig.6 DOS (a), band structure (b) and partial electron densities of the VBM at a 0.01 eV/Å^3 isosurface level (c) of $La_2Ti_2O_7$ with two N_s and one V_o defects s in a supercell calculated using HSE06 method. The dash line annotates the Fermi level.

In TiO_2, the N dopant concentration has an effect on the electronic structure of N-doped TiO_2[31]. If high concentration of N (*e.g.* 6.25 at%) was employed in the calculation, the N 2p state was mixed with O 2p, leading to band gap narrowing rather than localized deep energy state fromation[40]. If low concentration of N (*e.g.* 1.56 at%) was used in the calculation, a deep localized energy band formed in the forbidden band[31,34,35]. In order to study the influence of the nitrogen concentration on the electronic structure, we also investigated the DOS and band structure of $La_2Ti_2O_7$ with 7.1 at% of N concentration, corresponding to the system containing two N_S and one V_O in a supercell in Fig.1 (d). By comparing Fig.4 and Fig.7, it can be confirmed that solely doping N into $La_2Ti_2O_7$ led to the formation of a localized deep energy state in the forbidden gap, independent of the concentration change. For the two systems containing either two N_s (Fig.7 and Fig.S6) or two N_s plus one V_o (Fig.6 and Fig.S5), the electronic structures were very similar, except that the localized deep energy band disappeared completely in the latter case. This has further confirmed that the localized energy state can be removed and the band gap be narrowed simultaneously only when N_s and V_o co-exist in $La_2Ti_2O_7$.

In comparison with the systems containing N_S and N_S +Ti_i, the Ti 4d orbits contributed more to the VMB in $La_2Ti_2O_7$ containing both N_S and V_O, clearly demonstrated by the inserted DOS in Fig.6 (a). This indicated that orbits hybridization between non-metal and metal was enhanced in the case when N_S and V_O existed simultaneously, which can also be verified by the partial electron density of the VBM of $La_2Ti_2O_7$ containing different defects. In comparison with other configurations, strong orbits hybridization between N and Ti occurred in $La_2Ti_2O_7$ containing both N_S and V_O, as shown in Fig.6(c). The extended nature of the valence band edge caused by the hybridized N 2p and Ti 3d states is beneficial to the migration of photo-induced holes, which increases the oxidation power of the photocatalysts [31, 41]. As a result, the N doped $La_2Ti_2O_7$ nanosheets perform well in photocatalytic decomposition of methyl orange[13]. N doping is an effective method to realize the visible light photocatalytic activity. In short, if N doping in $La_2Ti_2O_7$ occurs in a reducing atmosphere, the presence of V_O will reduce the band gap and eliminate the localized energy band, leading to enhancement in the photocatalytic activity in both the ultraviolet and the visible light regions.

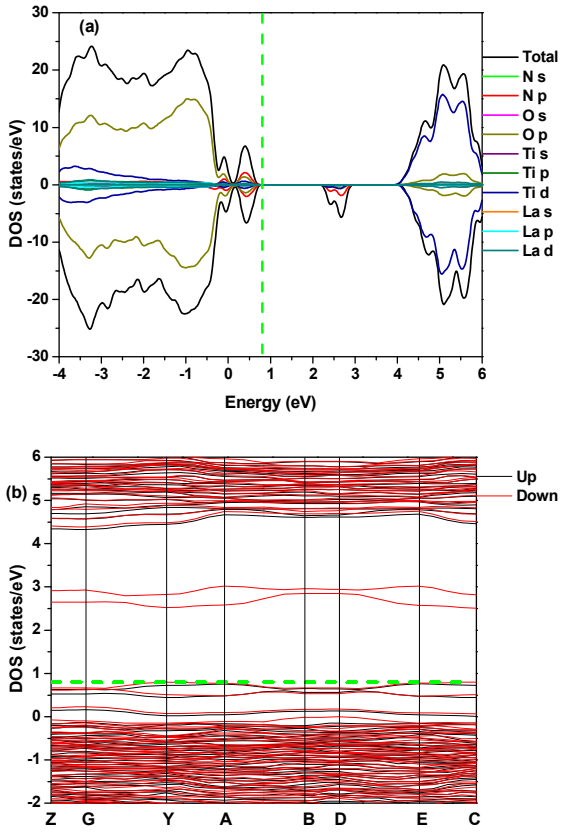

Fig. 7 DOS (a) and band structure (b) of $La_2Ti_2O_7$ with two N_s defects in a supercell calculated using HSE06 method. The dash line annotates the Fermi level.

4. Conclusions

The DFT and HSE06 hybrid methods were employed to investigate the influence of the N substitute doping co-existing with the oxygen vacancy and the interstitial Ti atom on the electronic structures. Solely doping N into $La_2Ti_2O_7$ caused the formation of the deep localized energy state, independent on the doping concentration. When interstitial Ti co-existed with N_S, the localized energy band was still present. However, when N_S co-existed with V_O, the localized energy state was completely removed and the band gap can be substantially narrowed. Further, the added DOS altered the VBM, which facilitated the migration of photo-induced holes and the oxidation power of the photocatalyst, introduced the direct transition at lower energy to increase light absorption. As a result, the N_S plus V_O model in $La_2Ti_2O_7$ can accurately interpret the fact that N doping into $La_2Ti_2O_7$ can not only lead to strong visible light photocatalytic activity but also enhance the performance under UV irradiation. This work reveals that tuning the non-neutral

point defects with the oxygen vacancy is an effective strategy for alleviating the problem associated with doping to increase light absorption, which have implication in engineering band gap of semiconductor photocatalysts.

Acknowledgements

This work was supported by Ph.D Program Foundation of the Ministry of Education of China (Grant No. 20121102110027), the National Science Foundation of China (Grant No. 51472013 and 91222110), the high-performance computing platform of Network Information Centre in Beihang University, and the National Computational Infrastructure (NCI) through the merit allocation scheme and used NCI resources and facilities in Canberra, Australia.

Notes and references

[a]Department of Physics, Beihang University, Beijing 100191, China. E-mail: zjy@buaa.edu.cn (J.Y. Zhang); Tel: +86-10-82315351; Fax: +86-10-82317931.

[b]Center for Clean Energy Technology, School of Chemistry and Forensic Science, University of Technology Sydney, PO Box 123, Broadway, Sydney, NSW 2007, Australia

[c]Department of Mechanical and Aerospace Engineering, West Virginia University, Morgantown, WV 26506-6106, USA. E-mail: nick.wu@mail.wvu.edu, Tel: +1-304-293-3326

1 K. Honda and A. Fujishima, *Nature*, 1972, **238**, 37.

2 H. Tong, S.X. Ouyang, Y. P. Bi, N. Umezawa, M. Oshikiri and J. H. Ye, *Adv. Mater.* 2012, **24**, 229.

3 J. Y. Li and N. Q. Wu, *Catal. Sci. Technol.* 2015, DOI: 10.1039/C4CY00974F.

4 A. Kudo and Y. Miseki, *Chem. Soc. Rev.*, 2009, **38**, 253.

5 H. G. Kim, D. W. Hwang, J. Kim, Y. G. Kim and J. S. Lee, *Chem. Comm.*, 1999,1077.

6 X. C. Wang, K. Maeda, A. Thomas, K. Takanabe, G. Xin, J. M. Carlsson, K. Domen and M. Antonietti, *Nature Mater.* , 2009, **8**, 76.

7 Y. Miseki, H. Kato and A. Kudo, *Energ. Environ. Sci.*, 2009, **2**, 306

8 R. Abe, M. Higashi, K. Sayama, Y. Abe and H Sugihara, *J. Phys Chem B*, 2006, **110**, 2219.

9 T. Takata, Y. Furumi, K. Shinohara, A.Tanaka, M. Hara, J. N. Kondo and K, Domen, *Chem. Mater.*, 1997, **9**,1063.

10 Y. F. Huang, Y. L. Wei, S. H. Cheng, L. Q. Fan,Y. B. Li, J. M. Lin and J. H. Wu, *Sol. Energ. Mater .Sol. Cells*, 2010, **94**, 761.

11 K.W. Li, Y. Wang, H. Wang, M.K. Zhu and Hui Yan, *Nanotechnology*, 2006, **17**, 4863.

12 Q. L. Yang, S. Z. Kang, H. Chen, W. B. Bu, J. Mu, *Desalination*, 2011, **266**, 149.

13 F. K. Meng, Z. L. Hong, J. Arndt, M. Li,M. J. Zhi, F. Yang and N.Q. Wu, *Nano Res*. 2012, **5**, 213.

14 Q. Wang, T. Hisatomi, Y.e Moriya, K. Maeda and K. Domen, *Catal. Sci. Technol*., 2013, **3**, 2098.

15 D. W. Hwang, H. G. Kim, J. S. Jang, S. W. Bae, S. M. Ji, J. S. Lee, *Catal. Today*, 2004, **93–95**, 845.

16 D. Arney, B. Porter, B. Greve, P. A. Maggard, *J. Photochem, Photobio A: Chem.*, 2008, **199**, 230.

17 D. W. Hwang , H. G. Kim, J. S. Lee, J. Kim , W.Li and S. H. Oh, *J. Phys. Chem. B*, 2005, **109**, 2093.

18 Z. M. Shao, S. Saitzek, P. Roussel, A. Ferri, Ol. Mentré and R. Desfeux, *CrystEngComm*, 2014. **16**, 8517.

19 A. Nashim, S. Martha and K. M. Parida, *RSC Adv*., 2014, **4**, 14633.

20 S.J. Hu, L.C. Jia, B. Chi, J. Pu and L. Jian, *J. Power Sources*, 2014, **266**, 304.

21 F. K. Meng, J. T. Li, Z. L. Hong, M. J. Zhi, A. Sakla, C. C. Xiang and N. Q. Wu, *Catal. Today*, 2013, **199**, 48

22 P. Liu, J. Nisar, B. Pathak and R. Ahuja, *Phys. Chem. Chem. Phys.*, 2013, **1**5, 17150.

23 P. Liu, J. Nisar, B. S. Sa, B. Pathak and Rajeev Ahuja, *J. Phys. Chem. C*, 2013, **117**, 13845.

24 G. Kresse and J. Furthmüller, *Phys. Rev. B:Condens. Matter Mater. Phys.*, 1996, **54**, 11169.

25 J. P. Perdew, K. Burke, and M. Ernzerhof, *Phys. Rev. Lett.*, 1996, **77**, 3865.

26 J. Heyd, G. E. Scuseria and Matthias Ernzerhof, *J. Chem. Phys.,* 2003, **118**, 8207.

27 G. Kresse and D. Joubert, *Phys. Rev. B:Condens. Matter Mater. Phys.*, 1999, **59**, 1758.

28 H. W. Schmalle, T. Williams and A. Reller, *Acta Cryst.*,1993. **B49**, 235.

29 L. J. Sham, M. Schlüter, *Phys. Rev. Lett.*, 1983, **51**, 1888.

30 L. J. Sham, M. Schlut, *Phys. Rev. B:Condens. Matter Mater. Phys.*, 1985, **32**, 3883.

31 N. Umezawa and J. H. Ye, *Phys. Chem. Chem. Phys.*,2012, **14**, 5924.

32 C. D. Valentin, G. Pacchioni and A. Selloni, *Phys. Rev. B:Condens. Matter Mater. Phys.*, 2004, **70**, 085116.

33 Z. Lin, A. Orlov, R. M. Lambert and M. C. Payne, *J. Phys. Chem. B*, 2005, **109** , 20948.

34 J. B. Varley, A. Janotti and C. G. Van de Walle, *Adv. Mater.*, 2011, **23**, 2343.

35 J. Wang, D. N. Tafen, J. P. Lewis, Z.L. Hong, A. Manivannan, M. J. Zhi , M. Li and N.Q. Wu, *J. Am. Chem. Soc.*, 2009, **131**, 12290.

36 C. D. Valentin , G. Pacchioni , A. Selloni , S. Livraghi and E. Giamello, *J. Phys. Chem. B*, 2005,**109**, 11414.

37 M. Batzill, E. H. Morales and U. Diebold, *Phys. Rev. Lett.*, 2006, **96**, 026103.

38 H. C. Wu, Y.S. Lin, and S.W. Lin, *Int. J. Photoenergy*, 2013, **2013**, 289328.

39 P. P. González-Borrero, H. S. Bernabé, N. G. C. Astrath, A. C. Bento, M. L. Baesso, M. V. Castro Meira, J. S. deAlmeida and A. Ferreira da Silva, *Appl. Phys. Lett*., 2011, **99**, 221909.

40 K. Aoki and Y. Taga, *Science*, 2001, **293**, 269.

41 H. Kawazoe, H.Yanagi, K. Ueda and H. Hosono, *MRS Bull*, 2000, **25**, 28.

